BULLETIN OF BIOMATHEMATICS

Bulletin of Biomathematics, 2024, 2(2), 182–197

https://www.bulletinbiomath.org
ISSN Online: 2980-1869 / Open Access
https://doi.org/10.59292/bulletinbiomath.2024008

RESEARCH PAPER

Bifurcations on a discrete–time SIS–epidemic model with saturated infection rate

Hasan S. Panigoro [1,*,‡], **Emli Rahmi** [1,‡], **Salmun K. Nasib** [1,‡], **Nur'ain Putri H. Gawa** [1,‡] **and Olumuyiwa James Peter** [2,‡]

[1]Biomathematics Research Group, Department of Mathematics, Universitas Negeri Gorontalo, Bone Bolango 96554, Indonesia, [2]Department of Mathematical and Computer Sciences, University of Medical Sciences, Ondo City, Ondo State, Nigeria

* Corresponding Author
‡ hspanigoro@ung.ac.id (Hasan S. Panigoro); emlirahmi@ung.ac.id (Emli Rahmi); salmun@ung.ac.id (Salmun K. Nasib); aingawa0802@gmail.com (Nur'ain Putri H. Gawa); peterjames4real@gmail.com (Olumuyiwa James Peter)

Abstract

In this paper, we explore the complex dynamics of a discrete-time SIS (Susceptible-Infected-Susceptible)-epidemic model. The population is assumed to be divided into two compartments: susceptible and infected populations where the birth rate is constant, the infection rate is saturated, and each recovered population has a chance to become infected again. Two types of mathematical results are provided namely the analytical results which consist of the existence of fixed points and their dynamical behaviors, and the numerical results, which consist of the global sensitivity analysis, bifurcation diagrams, and the phase portraits. Two fixed points are obtained namely the disease-free and the endemic fixed points and their stability properties. Some numerical simulations are provided to present the global sensitivity analysis and the existence of some bifurcations. The occurrence of forward and period-doubling bifurcations has confirmed the complexity of the solutions.

Keywords: SIS-epidemic model; saturated infection rate; bifurcation

AMS 2020 Classification: 37N25; 92B05; 39A60; 92D25

1 Introduction

The mathematical modeling using a deterministic approach is a powerful tool to reduce the impact of the infectious disease [1–3]. In recent decades, two popular ways are used for the deterministic approaches namely the continuous-time and the discrete-time models. There are many epidemiological studies employing differential equations for the operator of the continuous time model. See [4–9] and references therein. For the discrete-time model, the difference equation is used and becomes popular due to the complexity of the dynamical behaviors in epidemiological

➤ **Received:** 13.05.2024 ➤ **Revised:** 15.10.2024 ➤ **Accepted:** 23.10.2024 ➤ **Published:** 31.10.2024

cases. Most of them propose the complexity of dynamical behaviors such as period-doubling and Neimark-Sacker bifurcations as well as the existence of chaotic solutions. See [10–17] and cited articles therein.

The classical epidemic model is given by Kermack and MacKendrick [18, 19] defined by

$$\frac{dS}{dt} = -\beta SI,\ \frac{dI}{dt} = \beta SI - \rho I,\ \frac{dR}{dt} = \rho I, \tag{1}$$

where S is the susceptible compartment, I is the infected compartment, R is the recovered compartment, β is the infection rate, and ρ is the recovery rate. Some modifications are applied to include the real phenomena in nature. For example, Federico et al. [20] include the optimal vaccination and the recovery rate to the susceptible compartment to model (1). In another way, Zhang and Qiao [21] focus on studying the bifurcation analysis of model (5) by assuming the infection rate is saturated and the population has a strong Allee effect. Interesting works were also given by Li and Eskandari [1] which focus on the analytical and numerical results of a discrete-time seasonally forced SIR epidemic model. On the other hand, Omame et al. [22] and Atede et al. [23] have focused on investigating the application of model (1) on COVID-19 transmission by involving the vaccination and the memory effect. Some of them have integrated deterministic and stochastic approaches to describe the dynamical behaviors in modelling [24–30]. Following those articles, in this work, we also focus on the mathematical results of a modified SIR model and do not specifically discuss an epidemiological case. The model is modified based on some assumptions as follows:

(i) The constant birth rate is denoted by Λ.
(ii) The population has a natural death rate denoted by δ_1, δ_2, and δ_3 which respectively define the natural death rate of susceptible, infected, and recovered compartments.
(iii) The recovered individuals can be infected by disease again with the transfer rate to susceptible prey denoted by ω.
(iv) The infection rate term βSI is replaced by the saturated infection rate term denoted by $\frac{\beta SI}{\eta+I}$. This infection rate term naturally occurs in the epidemic model since each population can protect itself from infection so that although the infection population increases, the infection rate will have a threshold [31–33].

Thus, model (1) becomes

$$\frac{dS}{dt} = \Lambda - \frac{\beta SI}{\eta + I} - \delta_1 S + \omega R,\ \frac{dI}{dt} = \frac{\beta SI}{\eta + I} - \rho I - \delta_2 I,\ \frac{dR}{dt} = \rho I - \delta_3 R - \omega R. \tag{2}$$

By assuming all recovered compartments can be infected again, we drop the recovered compartment R and hence the model (2) is simplified into

$$\begin{aligned} \frac{dS}{dt} &= \Lambda - \frac{\beta SI}{\eta + I} + \omega I - \delta_1 S, \\ \frac{dI}{dt} &= \frac{\beta SI}{\eta + I} - (\omega + \delta_2)\, I. \end{aligned} \tag{3}$$

Now, we adopt similar ways as in [34–36] to construct the discrete-time model using the forward

Euler scheme. We get

$$\begin{aligned} \frac{S_{n+1}-S_n}{h} &= \Lambda - \frac{\beta S_n I_n}{\eta + I_n} + \omega I_n - \delta_1 S_n, \\ \frac{I_{n+1}-I_n}{h} &= \frac{\beta S_n I_n}{\eta + I_n} - (\omega + \delta_2) I_n. \end{aligned} \tag{4}$$

From model (4), the simplification yields

$$\begin{aligned} S_{n+1} &= S_n + h\left(\Lambda - \frac{\beta S_n I_n}{\eta + I_n} + \omega I_n - \delta_1 S_n\right), \\ I_{n+1} &= I_n + h\left(\frac{\beta S_n I_n}{\eta + I_n} - (\omega + \delta_2) I_n\right). \end{aligned} \tag{5}$$

Based on the above description, we get the key contributions and the novelty of this research are given as follows:

(i) The model is constructed using a saturated infection rate and all recovered individuals can be infected again. We also use the difference equation for the operator rather than the differential equation. According to our literature review, although the model is simple, we cannot find similar works as given by model (5).
(ii) All possible dynamical behaviors of fixed point are analyzed namely sink, source, saddle, and non-hyperbolic.
(iii) The most influential parameter concerning the basic reproduction number and the population density for each compartment is identified using the Partial Rank Correlation Coefficient (PRCC) along with Saltelli sampling to generate the data.
(iv) More complex dynamics are provided numerically namely the forward and period-doubling bifurcations.

We organize this article as follows: In Section 1, we give the introduction and model formulation. In Section 2, we explore the dynamical behaviors of the model by identifying the feasible fixed points, the basic reproduction number, and their stability properties. In Section 3, some numerical simulations are provided such as the global sensitivity analysis, forward, and period-doubling bifurcations by giving the PRCC bar chart, contour plots, PRCC time-series, bifurcation diagrams, and phase portraits around fixed points. We end this article by presenting a conclusion in Section 4.

2 Analytical results and findings

We start investigating the feasible fixed point of model (5) by solving the following equation

$$\begin{aligned} S &= S + h\left(\Lambda - \frac{\beta S I}{\eta + I} + \omega I - \delta_1 S\right), \\ I &= I + h\left(\frac{\beta S I}{\eta + I} - (\omega + \delta_2) I\right). \end{aligned} \tag{6}$$

We find two fixed points on the axial and the interior of the model (5) which are discussed in the next subsections.

The disease-free fixed point

The first fixed point is given by the disease-free fixed point (DFF) denoted by

$$E_0 = \left(\frac{\Lambda}{\delta_1}, 0\right),$$

which describes the condition when the disease disappears from the population. By following [37–41], we apply the next generation matrix to obtain the basic reproduction number ($\mathcal{R}_0$) which states the number of secondary infections caused by one primary infection in an entirely susceptible population. We get

$$\mathcal{R}_0 = \frac{\beta\Lambda}{(\omega+\delta_2)\,\delta_1\eta}. \tag{7}$$

Now, we give the following theorem to present the dynamical behaviors of DFF.

Theorem 1 *Let* $h_a = \frac{2}{\delta_1}$ *and* $h_b = \frac{2\omega}{(1-\mathcal{R}_0)(\omega+\delta_2)}$. *The DFF* $E_0 = \left(\frac{\Lambda}{\delta_1}, 0\right)$ *is*

(i) a sink (locally asymptotically stable) if $\mathcal{R}_0 < 1$ *and* $h < \min\{h_a, h_b\}$; *or*
(ii) a source if $\mathcal{R}_0 > 1$ *and* $h > h_a$; *or if* $\mathcal{R}_0 < 1$ *and* $h > \min\{h_a, h_b\}$; *or*
(iii) a saddle if $h < h_b$ *and* $\mathcal{R}_0 > 1$; *or if* $h < h_a$ *and* $\mathcal{R}_0 < 1$ *and* $h > h_b$; *or if* $h > h_a$ *and* $\mathcal{R}_0 < 1$ *and* $h < h_b$; *or*
(iv) a non-hyperbolic if $h = h_a$; *or* $\mathcal{R}_0 = 1$; *or* $\mathcal{R}_0 < 1$ *and* $h = h_b$.

Proof For DFF, we have the following Jacobian matrix:

$$J(S,I)|_{E_0} = \begin{bmatrix} 1-\frac{2h}{h_a} & \frac{(\delta_1\omega\eta-\beta\Lambda)h}{\delta_1\omega\eta} \\ 0 & 1-\frac{2h}{h_b} \end{bmatrix}.$$

Therefore, we obtain a pair of eigenvalues $\lambda_1 = 1-\frac{2h}{h_a}$ and $\lambda_2 = 1-\frac{2h}{h_b}$. By observing λ_1, we have the following condition

- $|\lambda_1| < 1$ when $h < h_a$; and
- $|\lambda_1| = 1$ when $h = h_a$; and
- $|\lambda_1| > 1$ when $h > h_a$.

We also have the sign of λ_2 as follows.

- $|\lambda_2| < 1$ when $\mathcal{R}_0 < 1$ and $h < h_b$; and
- $|\lambda_2| = 1$ when $\mathcal{R}_0 = 1$ or;
  when $\mathcal{R}_0 < 1$ and $h = h_b$; and
- $|\lambda_2| > 1$ when $\mathcal{R}_0 > 1$; or
  when $\mathcal{R}_0 < 1$ and $h > h_b$.

Following Lemma 1 in [42], all statements given by Theorem 1 are proven.

The endemic fixed point

The next fixed point is given by the endemic fixed point (EFP) defined by $\hat{E} = (\hat{S}, \hat{I})$ where $\hat{S} = \frac{(\omega+\delta_2)(\eta+\hat{I})}{\beta}$ and $\hat{I} = \frac{(\mathcal{R}_0-1)(\omega+\delta_2)\delta_1\eta}{\beta\delta_2+(\omega+\delta_2)\delta_1}$. The EFP describes the condition when the disease exists in the population where the existence condition is given by $\mathcal{R}_0 > 1$. To investigate the dynamics

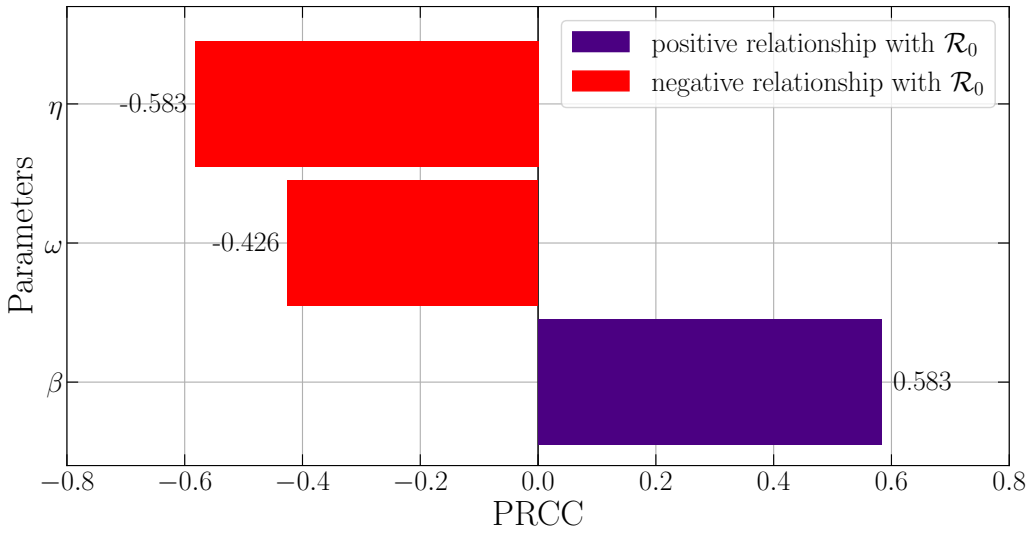

Figure 1. PRCC results with respect to the value of the basic reproduction number ($\mathcal{R}_0$). The infection rate (β) becomes the most influential parameter to the value of $\mathcal{R}_0$

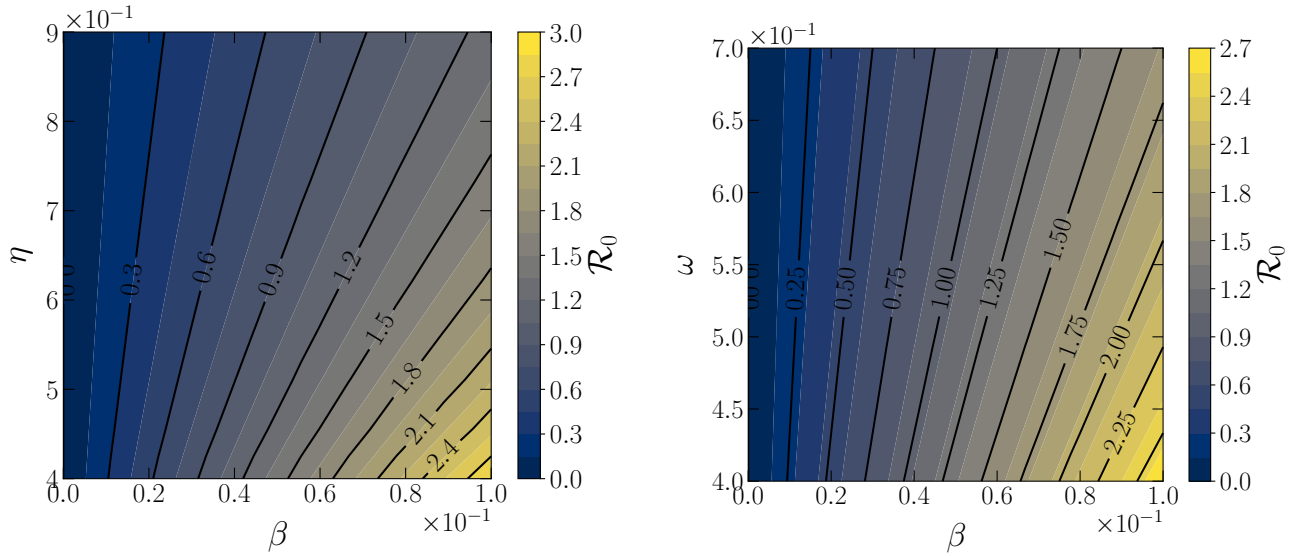

(a) Contour plot on $(\beta, \eta)-$plane

(b) Contour plot on $(\beta, \omega)-$plane

Figure 2. The contour plots of (a) (β, η), and (b) (β, ω) respect to the values of $\mathcal{R}_0$. The parameter β is directly proportional while η and ω is inversely proportional to $\mathcal{R}_0$

around EFP, we do linearization around EFP. The Jacobian matrix at EFP is given by

$$J(S,I)|_{\hat{E}} = \begin{bmatrix} 1 - h\left(\frac{(\beta+\delta_1)\hat{I}+\delta_1\eta}{\eta+\hat{I}}\right) & -h\left(\frac{\delta_2\eta-\omega\hat{I}}{\eta+\hat{I}}\right) \\ \frac{\beta\hat{I}h}{\eta+\hat{I}} & 1 - \frac{(\omega+\delta_2)\hat{I}h}{\eta+\hat{I}} \end{bmatrix},$$

and hence, we have eigenvalues

$$\lambda_{1,2} = \frac{1}{2}\left(\xi \pm \sqrt{\xi^2 - 4\zeta}\right), \tag{8}$$

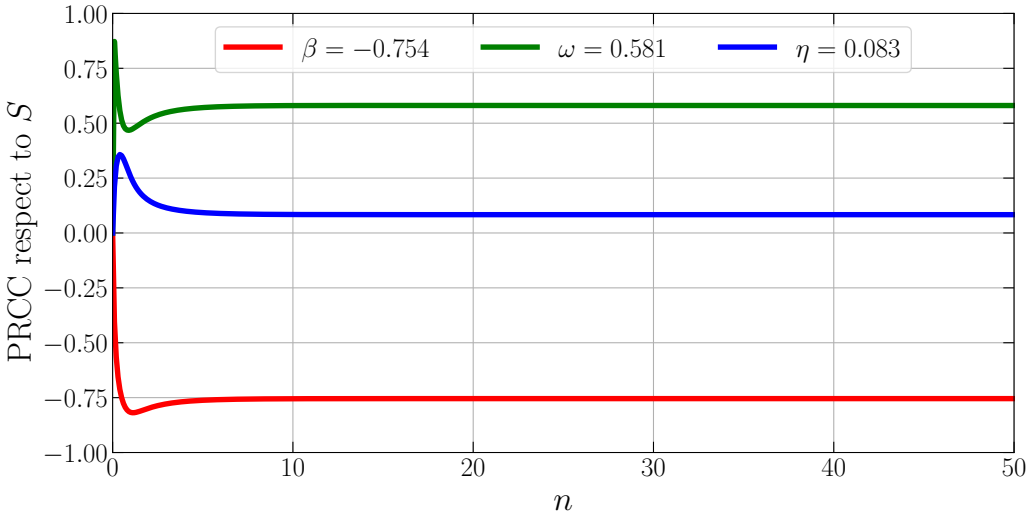

(a) PRCC respect to S

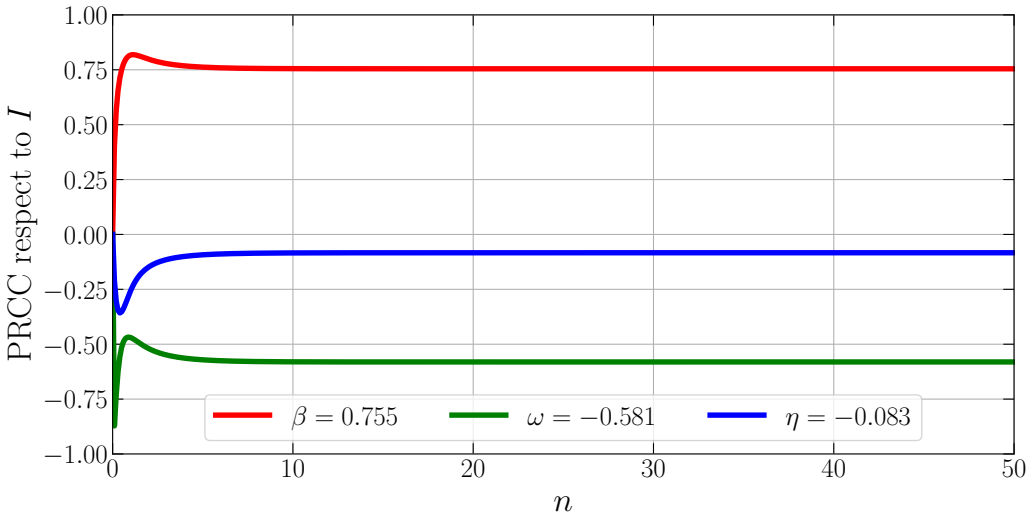

(b) PRCC respect to I

Figure 3. PRCC results respect to the density of susceptible individuals (S) and infected individuals (I). The parameter β is directly proportional to I and inversely proportional to S while *eta* and ω are opposite to it

where

$$\xi = 2 - \frac{h}{\eta + \hat{I}} \left[\left((\beta + \delta_1) - (\omega + \delta_2) \right) \hat{I} + \delta_1 \eta \right],$$

$$\zeta = 1 - \frac{h}{\eta + \hat{I}} \left[\left((\omega + \delta_2) + (\beta + \delta_1) \right) \hat{I} + \delta_1 \eta \right] + \frac{h^2 \hat{I}}{\eta + \hat{I}} \left[(\omega + \delta_2) \delta_1 + \beta \delta_2 \right].$$

Let $\Phi(\theta) = \theta^2 - \theta\xi + \zeta$. We have

$$\begin{aligned} \Phi(1) &= 1 - \xi + \zeta \\ &= \left[h \left((\omega + \delta_2) \delta_1 + \beta \delta_2 \right) - 2(\omega + \delta_2) \right] \frac{h\hat{I}}{\eta + \hat{I}}, \end{aligned}$$

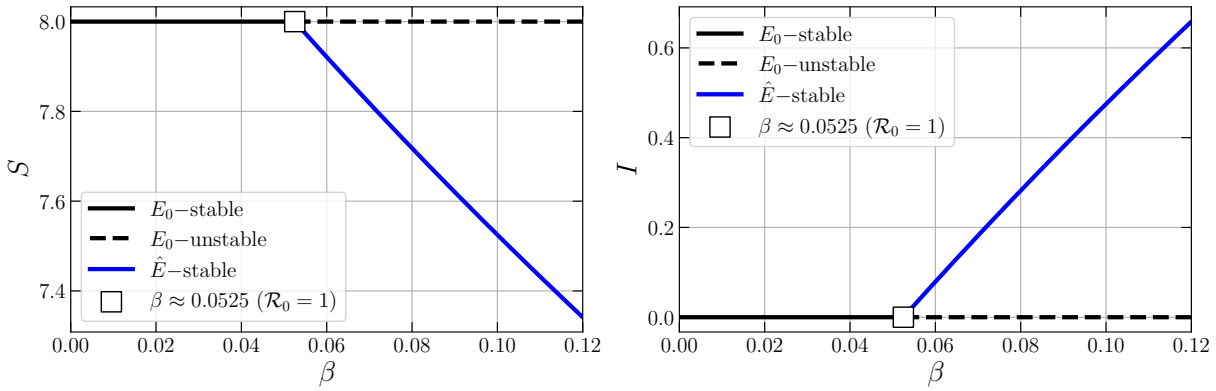

(a) Bifurcation diagram driven by β

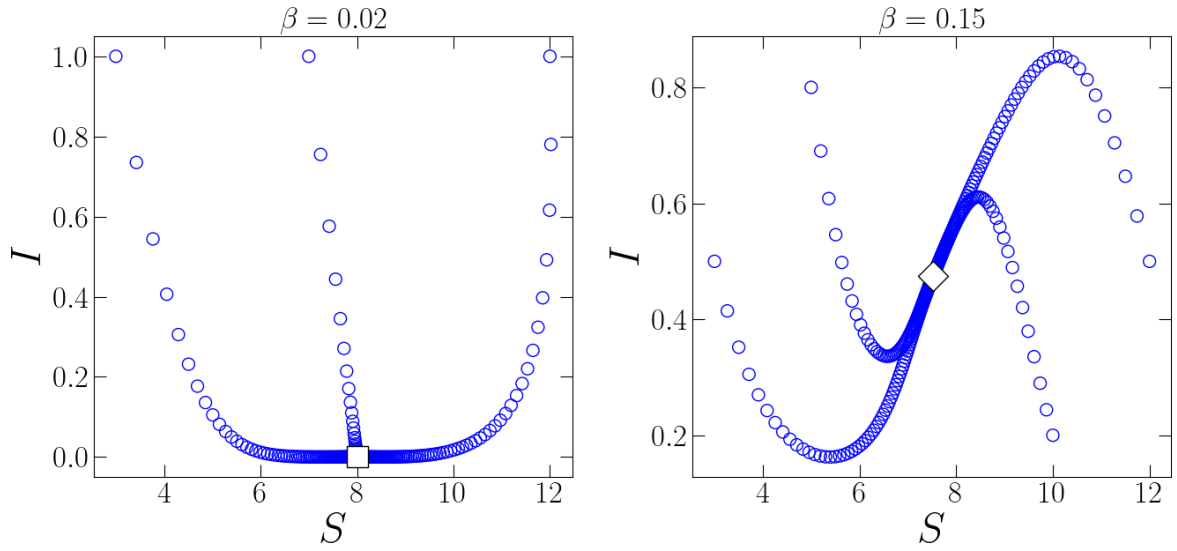

(b) Phase portrait for different values of β

Figure 4. Bifurcation diagrams and phase portraits of model (5) driven by β using parameter values: $\Lambda = 0.8$, $\eta = 0.6$, $\omega = 0.6$, $\delta_1 = 0.1$, $\delta_2 = 0.1$, and $h = 0.1$

which satisfies $\Phi(1) > 0$ when $h > \frac{2(\omega+\delta_2)}{(\omega+\delta_2)\delta_1+\beta\delta_2}$. We also achieve

$$\begin{aligned}\Phi(-1) &= 1 + \xi + \zeta \\ &= 4 - \frac{2h}{\eta + \hat{I}}\left[(\beta + \delta_1)\,\hat{I} + \delta_1\eta\right] + \frac{h^2\hat{I}}{\eta + \hat{I}}\left[(\omega + \delta_2)\,\delta_1 + \beta\delta_2\right].\end{aligned}$$

Following Lemmas 1 and 2 in [42], we have the following theorem as the results.

Theorem 2 *Let $\mathcal{R}_0 > 1$ and $h > \frac{2(\omega+\delta_2)}{(\omega+\delta_2)\delta_1+\beta\delta_2}$. The EFP is*

(i) a sink if $\Phi(-1) > 0$ and $\zeta < 1$; or
(ii) a source if $\Phi(-1) > 0$ and $\zeta > 1$; or
(iii) a saddle if $\Phi(-1) < 0$; or
(iv) a non-hyperbolic if $\Phi(-1) = 0$ and $\xi \neq 0, 2$; or if $\xi^2 < 4\zeta$ and $\zeta = 1$.

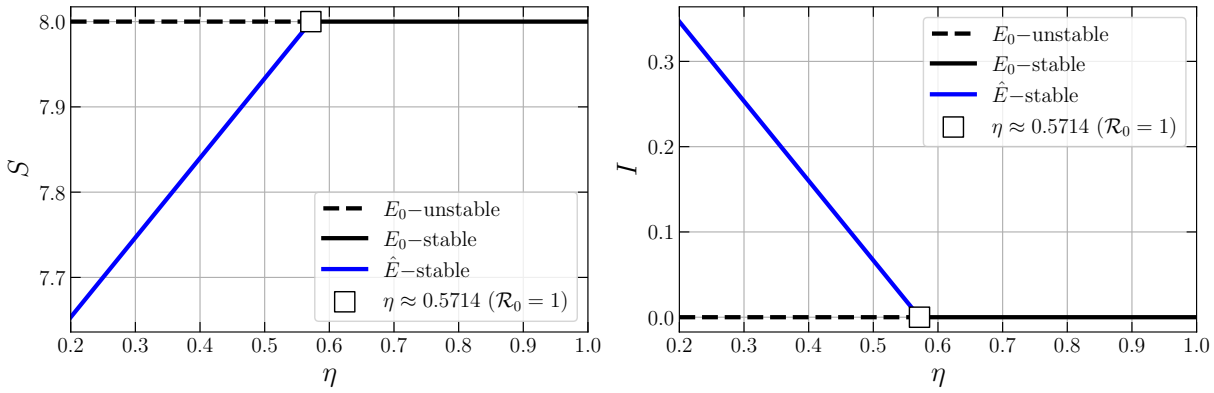

(a) Bifurcation diagram driven by η

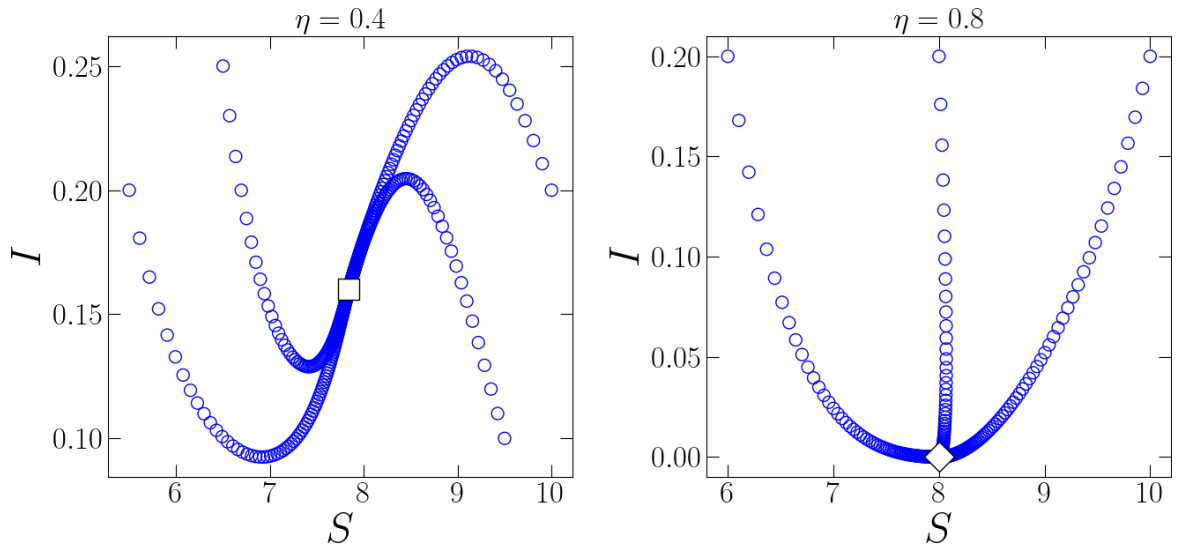

(b) Phase portrait for different values of η

Figure 5. Bifurcation diagrams and phase portraits of model (5) driven by η using parameter values: $\Lambda = 0.8$, $\beta = 0.05$, $\omega = 0.6$, $\delta_1 = 0.1$, $\delta_2 = 0.1$, and $h = 0.1$

3 Numerical results

To explore the complexity of the dynamical behaviors, some numerical simulations are demonstrated. Since no one specific epidemiological case is related to the model, we use hypothetical parameter values for the simulations. We first set the parameter values as follows.

$$\Lambda = 0.8,\ \beta = 0.01,\ \eta = 0.6,\ \delta_1 = 0.1,\ \delta_2 = 0.1,\ \omega = 0.6,\ h = 0.5. \tag{9}$$

By using the parameter values (9), we give the following subsections to show the global sensitivity analysis, forward, and period-doubling bifurcations.

Global sensitivity analysis

To investigate the most influential parameter of model (5), we perform the global sensitivity analysis [43, 44]. The Partial Rank Correlation Coefficient (PRCC) [45] is employed for parameter ranking along with Saltelli sampling [46] to generate the sample data around the parameter values given by (9). We consider the basic reproduction number and the population densities for the

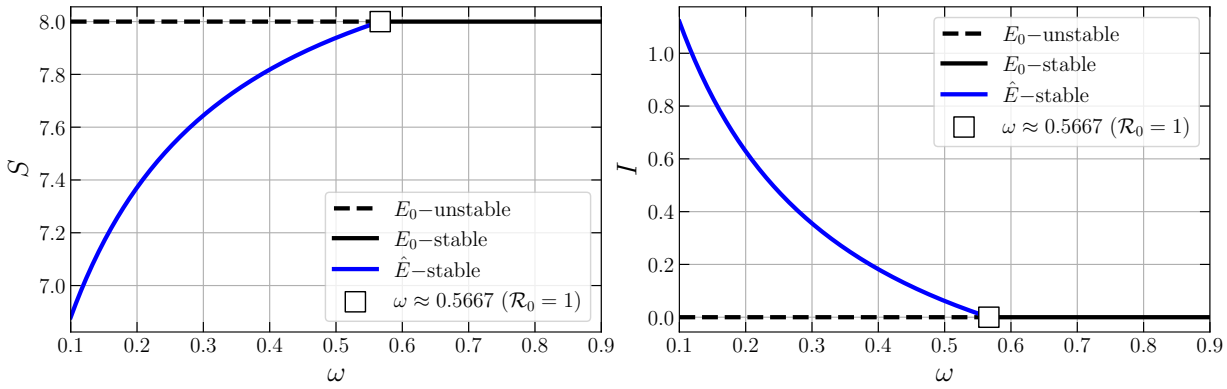

(a) Bifurcation diagram driven by η

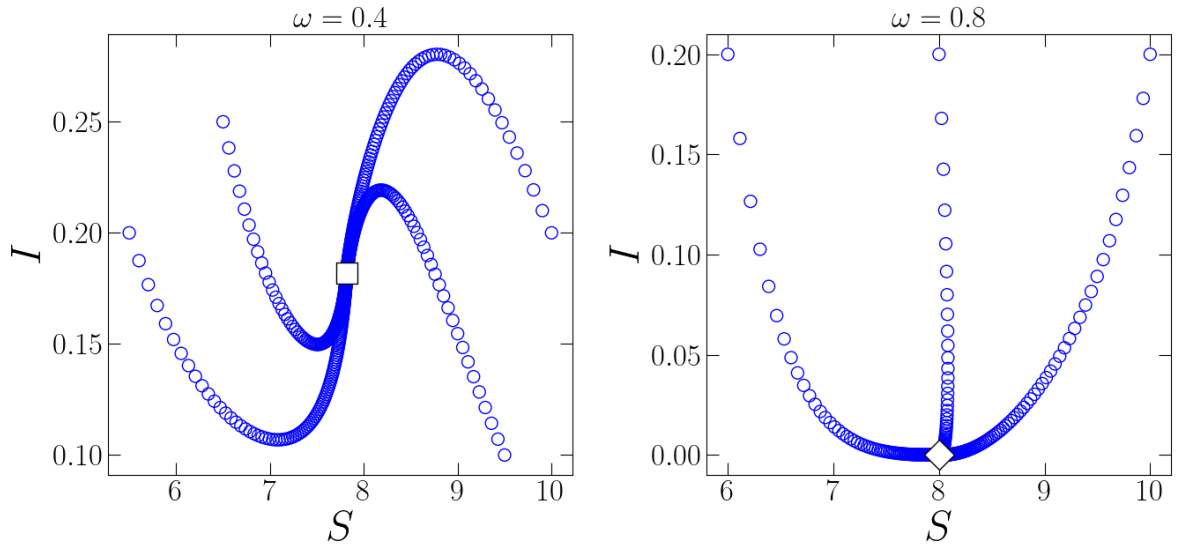

(b) Phase portrait for different values of ω

Figure 6. Bifurcation diagrams and phase portraits of model (5) driven by ω using parameter values: $\Lambda = 0.8$, $\beta = 0.05$, $\eta = 0.6$, $\delta_1 = 0.1$, $\delta_2 = 0.1$, and $h = 0.1$

constraint function and the rank of the parameter as the objective function. Since the birth rate (Λ) and the natural death rate δ_i, $i = 1, 2, 3$ can be obtained directly if the real data exists, we only focus on the impact of the infection rate (β), the recovery rate (ω), and the half-saturation constant (η).

We first investigate the most influential parameter of model (5) concerning the value of the basic reproduction number $(\mathcal{R}_0)$. As a result, we have the infection rate (β) become the most influential parameter with PRCC 0.583 while η and ω are respectively at the second and the third rank with PRCC -0.583 and -0.426. See the bar chart of PRCC results in Figure 1. We also confirm that β has a positive relationship with $\mathcal{R}_0$ while η and ω have a negative relationship with $\mathcal{R}_0$ by observing the sign of the PRCC results. This means that if the value of β increases, then the value of $\mathcal{R}_0$ increases. If the value of η or ω increases, the value of $\mathcal{R}_0$ will decrease. We give the contour plot of these conditions in Figure 2.

Now, we investigate the most influential parameter concerning the density of the susceptible compartment (S) and the infected compartment (I). Again, by applying PRCC and Saltelli sampling as well as computing the PRCC value for n in range $[0, 50]$, we find β still becomes the most influential parameter to the density of S and I. See the numerical results in Figure 3.

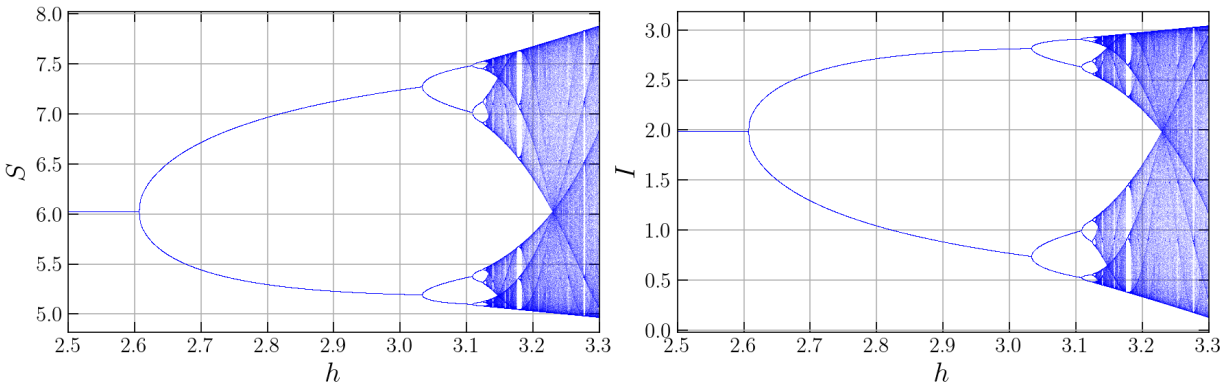

(a) Bifurcation diagram

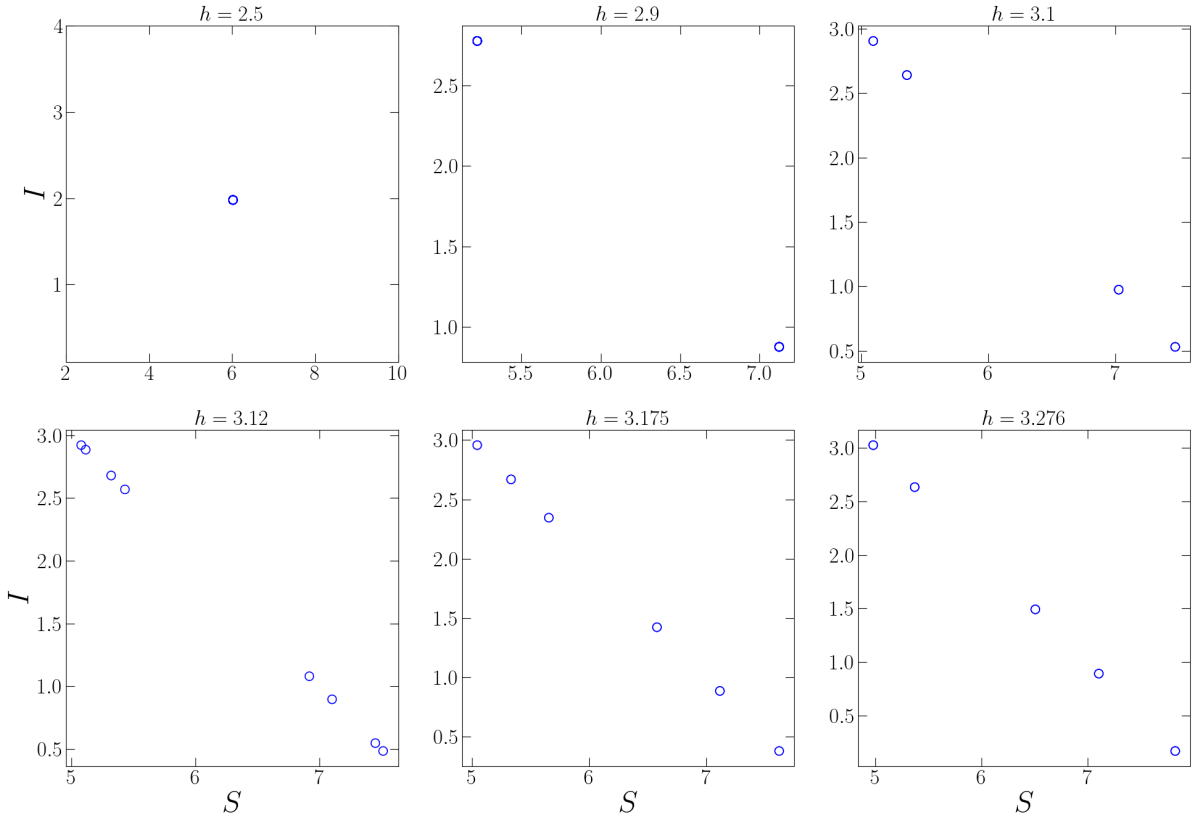

(b) Some periodic solutions

Figure 7. Bifurcation diagram and periodic solutions of model (5) driven by h using parameter values: $\Lambda = 0.8$, $\beta = 0.05$, $\eta = 0.6$, $\omega = 0.6$, $\delta_1 = 0.1$, $\delta_2 = 0.1$, and $h = 0.1$

From the sign of the PRCC values, we also verify that β has a negative relationship with S and a positive relationship with I, while η and ω have a positive relationship with S and a negative relationship with I. This means that when the infection rate increases, the density of the susceptible compartment decreases while the density of the infected compartment increases. When the recovery rate and the half-saturation constant increase, the density of the susceptible compartment increases, and the density of the infected compartment decreases.

Forward bifurcations

We then investigate the impact of the infection rate (β), the half-saturation constant (η), and the recovery rate (ω) on the dynamics of model (5). Let the parameter values as in (9). By varying

the value of β in the interval $[0, 0.12]$, we investigate the existence and stability condition for each fixed point. As a result, we have the bifurcation diagram as given in Figure 4(a) and phase portrait in Figure 4(b). When $\beta < \beta^*$ where $\beta^* \approx 0.0525$ (or $\mathcal{R}_0 \approx 1$), the nearby solution converges to DFF $E_0 = (8, 0)$ which indicate the DFF is a sink. When β crosses β^*, the DFF loses its stability followed by the occurrence of EFP $\hat{E}$ where the DFF becomes a saddle and EFP is a sink. This phenomenon is called forward bifurcation where β is the bifurcation parameter and β^* is the bifurcation point. Similar dynamical behaviors are presented when the half saturation parameter (η) and the recovery rate (ω) is varied. Using (9) and varying η in interval $[0.2, 1]$, we have a forward bifurcation where η and $\eta^* \approx 0.5714$ (or $\mathcal{R}_0 \approx 1$) are respectively the bifurcation parameter and bifurcation point. The forward bifurcation also occurs when ω crosses $\omega^* \approx 0.5667$ which confirms that ω and ω^* respectively become the bifurcation parameter and bifurcation point. See Figure 5 and Figure 6 for the numerical simulations of the bifurcation diagrams and their corresponding phase portraits. At these phenomena, we conclude that β, η, and ω have impacts on the existence and stability of DFE and FEP. The disease in the population will become extinct or endemic when the infection rate, half saturation constant, and the recovery rate are varied.

Period-doubling bifurcation

In this subsection, we present the occurrence of the sequence of period-doubling bifurcation as well as the example of the period of the solutions when the step-size (h). The parameter values given by (9) are set and h is varied in $[2.5, 3.3]$. As a result, we have Figure 7(a) as the bifurcation diagram. We confirm that the sink EFP becomes unstable when crosses $h \approx 2.61$ and a period-2 solution occurs. Each branch of the periodic solution also split into the other period-2 solution and so forth. This indicates the existence of the sequence of period-doubling bifurcation. We give Figure 7(b) to show some of the periodic solutions such as a sink for $h = 2.5$, period-2 for $h = 2.9$, period-4 for $h = 3.1$, period-8 for $h = 3.12$, period-6 for $h = 3.175$, and period-5 for $h = 3.276$. This phenomenon shows that the endemic point may lose its stability when the step-size becomes larger. Therefore, if we have less data for some interval of time, the dynamical behaviors may change via period-doubling bifurcation and the forecasting will be wrong.

4 Conclusion

The discrete-time SIS-epidemic model with a saturated infection rate has been studied. Some analytical and numerical results have been investigated. Two fixed points have been identified namely disease-free and endemic fixed points as well as the basic reproduction number. We have shown that the existence and stability of each fixed point depend on the basic reproduction number. More information about the dynamics of the model has been explored numerically. The PRCC along with Saltelli sampling has been used to investigate the most influential parameter concerning the value of the basic reproduction number and the density of each compartment which shows that the infection rate becomes the most influenced one. The existence of some bifurcations is also demonstrated namely forward bifurcations and period-doubling bifurcation. We conclude that the infection rate, the half-saturation constant, and the recovery rate have an impact not only on the stability of the fixed points but also on the occurrence of forward bifurcation. Although the model is mathematically explored such as the stability condition, sensitivity analysis, and some bifurcation phenomena, this work has less epidemiological interpretation since we do not apply this model to any epidemiological cases. Moreover, the model also studies two compartments only, which means we can explore more by adding some compartments based on the real phenomena in nature. This limitation will become interesting to study further.

Declarations

Use of AI tools

The authors declare that they have not used Artificial Intelligence (AI) tools in the creation of this article.

Data availability statement

All data generated or analyzed during this study are included in this article.

Ethical approval

The authors state that this research complies with ethical standards. This research does not involve either human participants or animals.

Consent for publication

Not applicable

Conflicts of interest

The authors declare that they have no conflict of interest.

Funding

This research was funded by Lembaga Penelitian dan Pengabdian Kepada Masyarakat-Universitas Negeri Gorontalo via PNBP-UNG with DIPA-UNG No. SP DIPA-023.17.2.677521/2023/2023, under contract No. B/704/UN47.D1/PT.01.03/2023.

Author's contributions

H.S.P.: Conceptualization, Methodology, Validation, Writing - Review & Editing, Supervision, Project Administration, Funding Acquisition. E.R.: Conceptualization, Methodology, Validation, Resources, Writing - Original Draft, Visualization, Supervision, Project Administration, Funding Acquisition. S.K.N.: Conceptualization, Formal Analysis, Resources, Writing - Original Draft N.P.H.G.: Software, Formal Analysis, Investigation, Data Curation, Writing - Original Draft, Visualization O.J.P.: Software, Validation, Investigation, Writing - Review & Editing. All authors discussed the results and contributed to the final manuscript.

Acknowledgements

The authors express their profound gratitude to the specialists who willingly imparted their knowledge and insights, which greatly aided in the creation of this manuscript.

References

[1] Li, B. and Eskandari, Z. Dynamical analysis of a discrete-time SIR epidemic model. *Journal of the Franklin Institute*, 360(12), 7989-8007, (2023). [CrossRef]

[2] Phukan, J. and Dutta, H. Dynamic analysis of a fractional order SIR model with specific functional response and Holling type II treatment rate. *Chaos, Solitons & Fractals*, 175(1), 114005, (2023). [CrossRef]

[3] Wu, P. and Feng, Z. Global dynamics of a space-age structured COVID-19 model coupling within-host infection and between-host transmission. *Communications in Nonlinear Science and Numerical Simulation*, 131, 107801, (2024). [CrossRef]

[4] Peter, O.J., Panigoro, H.S., Ibrahim, M.A., Otunuga, O.M., Ayoola, T.A. and Oladapo, A.O. Analysis and dynamics of measles with control strategies: a mathematical modeling approach. *International Journal of Dynamics and Control*, 11, 2538-2552, (2023). [CrossRef]

[5] Xu, C., Yu, Y., Ren, G., Sun, Y. and Si, X. Stability analysis and optimal control of a fractional-order generalized SEIR model for the COVID-19 pandemic. *Applied Mathematics and Computation*, 457, 128210, (2023). [CrossRef]

[6] Sadki, M., Harroudi, S. and Allali, K. Fractional-order SIR epidemic model with treatment cure rate. *Partial Differential Equations in Applied Mathematics*, 8, 100593, (2023). [CrossRef]

[7] Paul, A.K., Basak, N. and Kuddus, M.A. Mathematical analysis and simulation of COVID-19 model with booster dose vaccination strategy in Bangladesh. *Results in Engineering*, 21, 101741, (2024). [CrossRef]

[8] Centres, P.M., Perez-Morelo, D.J., Guzman, R., Reinaudi, L. and Gimenez, M.C. Diffusion model for the spread of infectious diseases: SIR model with mobile agents. *Physica A: Statistical Mechanics and its Applications*, 633, 129399, (2024). [CrossRef]

[9] Cui, W. and Zhao, Y. Saddle-node bifurcation and Bogdanov-Takens bifurcation of a SIRS epidemic model with nonlinear incidence rate. *Journal of Differential Equations*, 384, 252-278, (2024). [CrossRef]

[10] Hu, Z., Teng, Z. and Jiang, H. Stability analysis in a class of discrete SIRS epidemic models. *Nonlinear Analysis: Real World Applications*, 13(5), 2017-2033, (2012). [CrossRef]

[11] Din, Q. and Ishaque, W. Bifurcation analysis and chaos control in discrete-time eco–epidemiological models of pelicans at risk in the Salton Sea. *International Journal of Dynamics and Control*, 8, 132-148, (2020). [CrossRef]

[12] Szabadváry, J.H. and Zhou, Y. On qualitative analysis of a discrete time SIR epidemical model. *Chaos, Solitons & Fractals: X*, 7, 100067, (2021). [CrossRef]

[13] George, R., Gul, N., Zeb, A., Avazzadeh, Z., Djilali, S. and Rezapour, S. Bifurcations analysis of a discrete time SIR epidemic model with nonlinear incidence function. *Results in Physics*, 38, 105580, (2022). [CrossRef]

[14] Al-Basyouni, K.S. and Khan, A.Q. Discrete-time COVID-19 epidemic model with chaos, stability and bifurcation. *Results in Physics*, 43, 106038, (2022). [CrossRef]

[15] Ghosh, D., Santra, P.K., Mahapatra, G.S., Elsonbaty, A. and Elsadany, A.A. A discrete-time epidemic model for the analysis of transmission of COVID19 based upon data of epidemiological parameters. *European Physical Journal: Special Topics*, 231, 3461-3470, (2022). [CrossRef]

[16] He, Z.Y., Abbes, A., Jahanshahi, H., Alotaibi, N.D. and Wang, Y. Fractional-order discrete-time SIR epidemic model with vaccination: chaos and complexity. *Mathematics*, 10(2), 1-18, (2022). [CrossRef]

[17] Knopov, P.S. and Korkhin, A.S. Dynamic models of epidemiology in discrete time taking into account processes with lag. *International Journal of Dynamics and Control*, 11, 2193-2214, (2023). [CrossRef]

[18] Kermack, W.O. and McKendrick, A.G. A contribution to the mathematical theory of epidemics. *Proceedings of the Royal Society of London. Series A, Containing Papers of a Mathematical and Physical Character*, 115(772), 700-721, (1927). [CrossRef]

[19] Edelstein-Keshet, L. *Mathematical Models in Biology*. SIAM: Philadelphia, (2005). [CrossRef]

[20] Federico, S., Ferrari, G. and Torrente, M.L. Optimal vaccination in a SIRS epidemic model.

Economic Theory, 77, 49-74, (2024). [CrossRef]

[21] Zhang, J. and Qiao, Y. Bifurcation analysis of an SIR model with saturated incidence rate and strong Allee effect. *Journal of Biological Systems*, 32(01), 1-36, (2023). [CrossRef]

[22] Omame, A. and Abbas, M. The stability analysis of a co-circulation model for COVID-19, dengue, and zika with nonlinear incidence rates and vaccination strategies. *Healthcare Analytics*, 3, 100151, (2023). [CrossRef]

[23] Atede, A.O., Omame, A. and Inyama, S.C. A fractional order vaccination model for COVID-19 incorporating environmental transmission: a case study using Nigerian data. *Bulletin of Biomathematics*, 1(1), 78–110, (2023). [CrossRef]

[24] Kiouach, D. and Boulaasair, L. Stationary distribution and dynamic behaviour of a stochastic SIVR epidemic model with imperfect vaccine. *Journal of Applied Mathematics*, 2018, 1291402, (2018). [CrossRef]

[25] Coulibaly, B.D., Ghizlane, C. and El Khomssi, M. An approach to stochastic differential equations for long-term forecasting in the presence of α-stable noise: an application to gold prices. *Mathematical Modelling and Numerical Simulation with Applications*, 4(2), 165-192, (2024). [CrossRef]

[26] Boulaasair, L., Bouzahir, H., Vargas, A.N. and Diop, M.A. Existence and uniqueness of solutions for stochastic urban-population growth model. *Frontiers in Applied Mathematics and Statistics*, 8, 960399, (2022). [CrossRef]

[27] Aydın, N.S. A seismic-risk-based bi-objective stochastic optimization framework for the pre-disaster allocation of earthquake search and rescue units. *Mathematical Modelling and Numerical Simulation with Applications*, 4(3), 370-394, (2024). [CrossRef]

[28] Yavuz, M., Coşar, F.Ö., Günay, F. and Özdemir, F.N. A new mathematical modeling of the COVID-19 pandemic including the vaccination campaign. *Open Journal of Modelling and Simulation*, 9(3), 299-321, (2021). [CrossRef]

[29] Boulaasair, L. Threshold properties of a stochastic epidemic model with a variable vaccination rate. *Bulletin of Biomathematics*, 1(2), 177–191, (2023). [CrossRef]

[30] Yavuz, M., Boulaasair, L., Bouzahir, H., Diop, M.A. and Benaid, B. The impact of two independent Gaussian white noises on the behavior of a stochastic epidemic model. *Journal of Applied Mathematics and Computational Mechanics*, 23(1), 121–134, (2024). [CrossRef]

[31] Bentaleb, D., Harroudi, S., Amine, S. and Allali, K. Analysis and optimal control of a multi-strain SEIR epidemic model with saturated incidence rate and treatment. *Differential Equations and Dynamical Systems*, 31(4), 907-923, (2023). [CrossRef]

[32] Sun, D., Li, Q. and Zhao, W. Stability and optimal control of a fractional SEQIR epidemic model with saturated incidence rate. *Fractal and Fractional*, 7(7), 533, (2023). [CrossRef]

[33] Bounkaicha, C. and Allali, K. Modelling disease spread with spatio-temporal fractional derivative equations and saturated incidence rate. *Modeling Earth Systems and Environment*, 10, 259-271, (2024). [CrossRef]

[34] Ahmed, R., Rafaqat, M., Siddique, I. and Arefin, M.A. Complex dynamics and chaos control of a discrete-time predator-prey model. *Discrete Dynamics in Nature and Society*, 2023, 8873611, (2023). [CrossRef]

[35] Hamada, M.Y., El-Azab, T. and El-Metwally, H. Bifurcation analysis of a two-dimensional discrete-time predator–prey model. *Mathematical Methods in the Applied Sciences*, 46(4), 4815-4833, (2023). [CrossRef]

[36] Panigoro, H.S., Resmawan, R., Rahmi, E., Beta, M.A. and Sidik, A.T.R. The existence of a limit-cycle of a discrete-time Lotka-Volterra model with fear effect and linear harvesting. In Proceedings, *E3S Web of Conferences* (Vol. 400), p. 03003, (2023, July). [CrossRef]

[37] Anggriani, N., Tasman, H., Ndii, M.Z., Supriatna, A.K., Soewono, E. and Siregar, E. The effect of reinfection with the same serotype on dengue transmission dynamics. *Applied Mathematics and Computation*, 349, 62-80, (2019). [CrossRef]

[38] Banni, E.M., Kleden, M.A., Lobo, M. and Ndii, M.Z. Estimasi reproduction number model matematika penyebaran malaria di Sumba Tengah, Indonesia. *Jambura Journal of Biomathematics (JJBM)*, 2(1), 13-19, (2021). [CrossRef]

[39] Moya, E.M.D., Pietrus, A. and Oliva, S.M. Mathematical model with fractional order derivatives for Tuberculosis taking into account its relationship with HIV/AIDS and Diabetes. *Jambura Journal of Biomathematics (JJBM)*, 2(2), 80-95, (2021). [CrossRef]

[40] Kumari, N., Kumar, S., Sharma, S., Singh, F. and Parshad, R. Basic reproduction number estimation and forecasting of COVID-19: A case study of India, Brazil and Peru. *Communications on Pure & Applied Analysis*, 22(2), 417-440, (2023). [CrossRef]

[41] Muzembo, B.A., Kitahara, K., Mitra, D., Ntontolo, N.P., Ngatu, N.R., Ohno, A. et al. The basic reproduction number (R_0) of ebola virus disease: A systematic review and meta-analysis. *Travel Medicine and Infectious Disease*, 57, 102685, (2024). [CrossRef]

[42] Panigoro, H.S., Rahmi, E., Achmad, N., Mahmud, S.L., Resmawan, R. and Nuha, A.R. A discrete-time fractional-order Rosenzweig-Macarthur predator-prey model involving prey refuge. *Communications in Mathematical Biology and Neuroscience*, 2021, 77, (2021). [CrossRef]

[43] Nayeem, J., Podder, C.N. and Salek, M.A. Sensitivity analysis and impact of an imperfect vaccine of two strains of Hepatitis B virus infection. *Journal of Biological Systems*, 31(02), 437-458, (2023). [CrossRef]

[44] Lu, X. and Borgonovo, E. Global sensitivity analysis in epidemiological modeling. *European Journal of Operational Research*, 304(1), 9-24, (2023). [CrossRef]

[45] Marino, S., Hogue, I.B., Ray, C.J. and Kirschner, D.E. A methodology for performing global uncertainty and sensitivity analysis in systems biology. *Journal of Theoretical Biology*, 254(1), 178-196, (2008). [CrossRef]

[46] Saltelli, A. Making best use of model evaluations to compute sensitivity indices. *Computer Physics Communications*, 145(2), 280-297, (2002). [CrossRef]

Bulletin of Biomathematics (BBM)
(https://bulletinbiomath.org)

How to cite this article: Panigoro, H.S., Rahmi, E., Nasib, S.K., Gawa, N.P.H. & Peter, O.J. (2024). Bifurcations on a discrete-time SIS-epidemic model with saturated infection rate. *Bulletin of Biomathematics,* 2(2), 182-197. https://doi.org/10.59292/bulletinbiomath.2024008